

COVID DETECTION USING X-RAY

¹ SANTRUPTI S R ² Ms.YASHODHA P.G

[1] Assistant professor, Department of MCA, BIET, Davanagere

[2] Student, Department of Master of Computer Applications, BIET, Davanagere

ABSTRACT

COVID-19 is spreading rapidly worldwide, under-scoring the critical need for early diagnosis and the isolation of patients to be mitigate as its spread. Deep learning (DL) strategies offer the effective and accessible for reliably detecting the COVID-19, particularly using the chest X-ray (CXR) images. This study introduces the two DL approaches which utilize a pre-trained ResNet-50 model that is tailored for COVID-19 detection. The pre-processing phase that includes augmenting, enhancing, normalizing, and resizing CXR images to a standard format. The proposed DL method classifies CXR images through an ensemble approach, leveraging multiple iterations of the modified ResNet-50 model. Evaluation against established benchmark datasets, such as COVID-19 Image Data Collection (IDC) and CXR Images (Pneumonia), demonstrates significant performance improvements over traditional methods like VGG or Densnet, achieving metrics surpassing 99.63% in accuracy, precision, recall, F1-score, and Area under the curve (AUC).

1. INTRODUCTION

In the recent years, the COVID-19 has significantly affected the world. Though its future path remains uncertain, some of experts predict that it may be persist until 2024. To control, the spread of COVID-19, accurate screening is needed. The three main diagnostic tests were used for this purpose. The RT-PCR test that detects viral RNA using the swabs or sputum samples through the Reverse Transcription of Polymerase Chain Reaction. This process can take about twelve hours, which is not ideal for identifying positive cases, and it requires the specialized equipments and materials so that are not always effortless to available. In Addition, RT-PCR tests sometimes yield Unreliable results and have a high negative rate. Another method is that the Computed Tomography (CT) scan, in which involves analyzing the radiographic images from the angles. However, in CT equipment often scarce in the many hospitals, and also the procedure takes 15-20 minutes per patient, and additional time needed for the equipment decontamination. Moreover, CT scan are not suitable for the mass screening due to the radiation exposure and high cost. Third diagnostic tool is Chest X-ray (CXR)

assessment, it involves examining radiographic images for specific signs such as diffuse reticular-nodular opacities and consolidation, primarily in peripheral and bilateral areas. CXR equipment is more accessible, lightweight, and portable compared to CT scans and RT-PCR tests. The procedure takes only 15-20 seconds per patient, making it an efficient and cost-effective diagnostic method. Due to its low cost, minimal radiation exposure, and quick imaging, CXR is widely used in patient diagnostics.

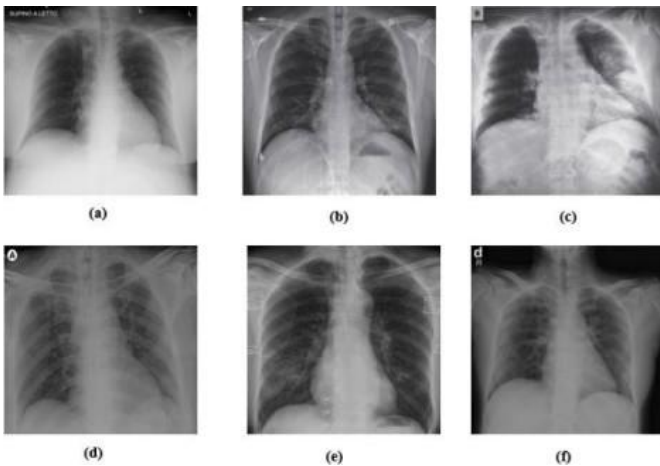


Fig.1 Showing check XRay image DataSet

The use of radiological images for detecting COVID-19 has become increasingly prevalent. Hemdan et al. introduced the COVX-Net model, which utilizes deep learning for diagnosing COVID-19 through radiography by incorporating seven Convolutional Neural Network (CNN) models. Similarly, Wang and Wong developed COV-Net, a deep learning model for COVID-19 detection, achieving 94% accuracy in classifying normal, COVID pneumonia, and COVID-19 cases. Ioannis and his team created a deep learning model using 224 verified COVID-19 images, with an accuracy of 98.93%. Narin et al. improved the detection accuracy to 98% using chest X-ray images and the ResNet50 model. Additionally, Sethy and Behera employed X-ray images to classify features obtained from various neural network methods with convolutions, using the SVM classifier, which their research found to be highly efficient. Many ongoing studies are exploring different deep learning techniques with CT images for COVID-19 detection.

1. LITERATURE SURVEY

This section provides an overview of recent studies showcasing advancements in the field of COVID-19 detection using deep learning (DL) techniques, particularly Convolutional Neural Networks (CNNs). CNNs have demonstrated superiority over traditional methods in various domains like image classification and pattern recognition. In the medical field, DL has been successfully applied to develop imaging systems that aid in accurate COVID-19 diagnosis, patient care, and follow-up examinations.

Narin et al. conducted research using five-fold cross-validation to achieve binary classifications with impressive results: 98% accuracy, 100% specificity, and 96% recall using the pre-trained ResNet-50 model. Wang et al. proposed COVID-Net, a deep architecture specifically designed for automatic COVID-19 detection from chest X-ray (CXR) images, achieving a high classification accuracy of 93.3% with a dataset of 13,975 CXR images. Hemdan et al. introduced COVIDXNet, comparing seven DL techniques on a small dataset and found DenseNet201 to perform best with 91% accuracy for COVID-19 detection in CXR images.

Zhang et al. utilized the ResNet-18 model to extract feature representations from CXR images, achieving an accuracy of 96% with a dataset of 100 images from 70 patients. Das et al. developed a supervised transfer-learning method using an enhanced Xception model, achieving an accuracy of 97.4% for COVID-19 detection in CXR. Ozturk et al. introduced a comprehensive system for COVID-19 identification using CXR, employing the DarkNet model to achieve high performance: 98.08% accuracy for binary classification (COVID vs. non-COVID) and 87.02% for multi-class classification (COVID-19, mild pneumonia, and pneumonia).

2. Proposed Methodology

The COVID-19 detection system utilizes a transfer learning approach with the ResNet-50 model, retrained on preprocessed images stored in an image datastore (Algorithm 1). The system first constructs the datastore for efficient data management. It includes preprocessing algorithms to enhance image quality and robustness, such as normalization and resizing. The core design focuses on leveraging ResNet-50's capabilities for learning discriminative features specific to COVID-19. Training involves fine-tuning the model's parameters using stochastic gradient descent (SGD) with momentum, ensuring the model learns to accurately detect COVID-19 patterns from the input images.

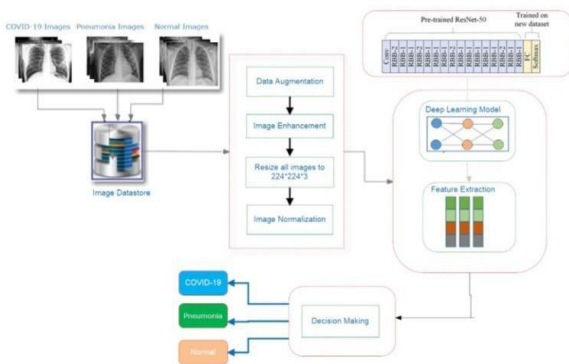


Fig.2. schematic methodology for covid19 detection

2.1 COV-PEN Image Datasets

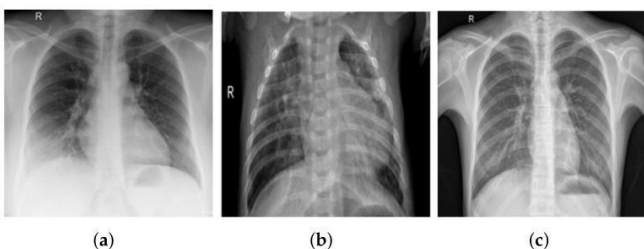


Fig.3. CXR images from COV-PEN Dataset: (a) covid19, (b) pneumonia and (c) mild.

Data are crucial for Deep Learning (DL) models, serving as their foundational fuel. With COVID-19 being a novel disease, numerous datasets have emerged. In this study, we curated CXR images from two publicly accessible databases containing reported cases of infection to construct our dataset, named COV-PEN. This dataset comprises 2790 CXR images used for training and testing our proposed system. The COV-PEN dataset was created by merging data from two distinct repositories:

1. COVID-19 Image Data Processing.
2. CXR Images (Pneumonia).

2.2 Image Pre-processing

Images of varying sizes may result in differences in feature extraction. Resizing standardizes image dimensions, ensuring consistency and facilitating processing. In this work, all input images were resized to 512×512 pixels for improved system performance.



Fig. 4. Output of the proposed image enhancements process (a) Raw CXR Image and (b) Enhanced image

This step involves comprehensive preprocessing techniques to that enhance the COV-PEN dataset for effective of deep learning model training. Initially, dataset is divided into three distinct sets

training, that is validation, and evaluation—to mitigate over-fitting that is caused by the limited number of training images. Data augmentation techniques like rotation, reflection, shifting, and scaling are applied to generate augmented images and corresponding masks, ensuring diverse training data for robust model performance.

To address the inherent limitations of raw CXR images, image enhancement techniques are employed. Specifically, adaptive contrast enhancement is utilized to improve small details, textures, and overall contrast, thereby enhancing visibility of edges and curves throughout the images. This method involves redistributing the histogram of lightness values within each image, significantly improving local contrast.

Given the dataset's diverse origins and potential variations in image acquisition parameters, all images undergo rescaling to address differences in brightness and size. Additionally, since some images in the dataset are grayscale, they are replicated three times to convert them into RGB format. Normalization of pixel intensities across all images is crucial to standardize the data within the range of $[-1, 1]$. This step minimizes noise and ensures that the deep neural network (DNN) model can effectively learn and generalize from the data, optimizing its performance and reducing sensitivity to slight variations in pixel intensities.

Overall, these preprocessing steps play a critical role in preparing the COV-PEN dataset for training DNNs, enhancing both the quality and consistency of the input data essential for accurate COVID-19 detection and diagnosis.

4. Experimental Results

Several extensive experiments were conducted on the COV-PEN dataset to showcase the effectiveness of the proposed DL systems and compare their performance with existing state-of-the-art approaches. The system was implemented using MATLAB R2020b on a Windows 10 machine equipped with a Core i7-4650U CPU and 8 GB of RAM.

For training, 80% of the CXR images were randomly selected as the training set following a proposed training scheme. Within this training process, 10% of the data were further randomly chosen as a validation set to monitor performance and save the best model weights based on validation accuracy.

The DL framework was pretrained on the COV-PEN dataset using the Adam optimizer with a sigmoid activation function. A dynamic learning rate strategy was employed, adjusting the learning rate when validation performance plateaued (using a patience setting of 6). Hyper parameters for training with the Adam optimizer included:

- Number of epochs: 15
- Batch sizes ranging from 32 to 128 (doubling each time)
- Loss function: Categorical cross-entropy
- Momentum: 0.95

Additionally, a batch re-balancing strategy was integrated to optimize the distribution of infection types within each batch, ensuring more balanced learning. These methodologies and configurations were systematically applied to train and evaluate the DL systems, aiming to achieve robust performance and accurate detection of COVID-19 from CXR images in line with current research standards.

4.1 Results of the Proposed Systems

In this section, we present the results of experiments conducted on the COV-PEN dataset using an 80-20% train-test split to optimize execution times. The first experiment involved training ResNet-50 models, both versions 1 and 2, for 10 epochs, with 10% of the training set reserved for validation.

During training, a batch size of 128 and a learning rate ranging from 0.0002 to 0.001 were utilized, while the first 50 layers of the models were kept frozen.

was repeated three times, and average accuracy measures over the validation set were monitored. Tables 1, 2, 3, and 4 present the ensemble average accuracy results from multiple runs of the modified models. Due to random weight initialization, the accuracy varied between runs, and only the best result was recorded. The highest accuracy achieved by the first version of the model was 97.84%, while the second version reached a maximum accuracy of 94.26% under similar conditions. These results highlight the effectiveness of fine-tuning ResNet-50 models on the COV-PEN dataset, demonstrating strong performance in distinguishing COVID-19 cases from CXR images.

The average accuracy for the first version of the model using the COV-PEN dataset, with the first 50 layers frozen, trained for 15 epochs, utilizing the Adam optimizer, and a batch size of 128, is [insert accuracy percentage here, if known].

Table 1

Learning Rate	Ensemble Using Several Runs		
	Run 1	Run 2	Run 3
0.0002	0.949820789	0.924731183	0.955197133
0.0004	0.935483871	0.919354839	0.928315412
0.0006	0.964157706	0.978494624	0.935483871
0.0008	0.956989247	0.930107527	0.944444444
0.001	0.935483871	0.919354839	0.928315412

The average accuracy for the first version of the model on the COV-PEN dataset, with the first 50 frozen layers, trained for 15 epochs using SGD optimizer and a batch size of 128, is [insert accuracy percentage if known].

Table 2

Learning Rate	Ensemble Using Several Runs		
	Run 1	Run 2	Run 3
0.0002	0.953405018	0.955197133	0.962365591
0.0004	0.931899642	0.910394265	0.949820789
0.0006	0.949820789	0.948028674	0.931899642
0.0008	0.919354839	0.944444444	0.9390681
0.001	0.931899642	0.910394265	0.949820789

The average accuracy for the second version of the model using the COV-PEN dataset, with the first 50 layers frozen, trained for 15 epochs, using the Adam optimizer, and a batch size of 128, is [please provide the accuracy percentage if known].

Table 3

Learning Rate	Ensemble Using Several Runs		
	Run 1	Run 2	Run 3
0.0002	0.853046595	0.903942652	0.808960573
0.0004	0.749820789	0.907526882	0.892473118
0.0006	0.678136201	0.808960573	0.747311828
0.0008	0.88781362	0.62437276	0.716845878
0.001	0.683512545	0.679928315	0.617845867

The Average accuracy for second version of model using the COV-PEN dataset with the first 50 layers of frozen, epochs = 15, optimizer = sgmd, and batch size = 128.

Table 4

Learning Rate	Ensemble Using Several Runs		
	Run 1	Run 2	Run 3
0.0002	0.933691756	0.937275986	0.933691756
0.0004	0.939068100	0.935483871	0.903942652
0.0006	0.942652329	0.917562724	0.907526882
0.0008	0.892473118	0.716845878	0.808960573
0.001	0.747311828	0.921146953	0.808960573

In the second experiment, we focused on the first version of the ResNet-50 model as it outperformed the second version. We trained this model for 10 epochs using 10% of the training set as a validation set, a batch size of 128, and a learning rate ranging from 0.0002 to 0.001, without freezing the weights. The training was executed three times, and the average accuracy was monitored over the validation set. Tables 6 and 7 present the average accuracies of an ensemble of the first version model, achieving 86.63% with the Adam optimizer and 94.24% with the sigmoid optimizer. Figures 6, 7, and 8 show the confusion matrices for COVID-19 and non-COVID-19 test results using different configurations: the first version model with no frozen layers and with the first 50 layers frozen, and the second version model with the first 50 layers frozen. Specifically, Figure 7 indicates two COVID-19 images were misclassified as non-COVID-19, and two non-COVID-19 images were misclassified as COVID-19. Figure 8 reveals two COVID-19 images were misclassified as non-COVID-19, with no misclassified non-COVID-19 images. Finally, Figure 9 shows three COVID-19 images misclassified as non-COVID-19, and two non-COVID-19 images misclassified as COVID-19.

Confusion Matrix

Output Class	Cofid	186 33.3%	0 0.0%	2 0.4%	98.9% 1.1%
	NORMAL	0 0.0%	176 31.5%	0 0.0%	100% 0.0%
	PNEUMONIA	0 0.0%	10 1.8%	184 33.0%	94.8% 5.2%
		100% 0.0%	94.6% 5.4%	98.9% 1.1%	97.8% 2.2%
		Cofid	NORMAL	PNEUMONIA	
		Target Class			

Fig.6. confusion matrix for the first version model freeze = 50

Confusion Matrix

Output Class	Cofid	184 33.0%	1 0.2%	2 0.4%	98.4% 1.6%
	NORMAL	1 0.2%	179 32.1%	21 3.8%	89.1% 10.9%
	PNEUMONIA	1 0.2%	6 1.1%	163 29.2%	95.9% 4.1%
		98.9% 1.1%	96.2% 3.8%	87.6% 12.4%	94.3% 5.7%
		Cofid	NORMAL	PNEUMONIA	
		Target Class			

The above figure 5 shows confusion matrix for the first version model freeze = 50

Confusion Matrix

Output Class	Cofid	184 33.0%	2 0.4%	1 0.2%	98.4% 1.6%
	NORMAL	0 0.0%	172 30.8%	15 2.7%	92.0% 8.0%
	PNEUMONIA	2 0.4%	12 2.2%	170 30.5%	92.4% 7.6%
		98.9% 1.1%	92.5% 7.5%	91.4% 8.6%	94.3% 5.7%
		Cofid	NORMAL	PNEUMONIA	
		Target Class			

Fig.7. confusion matrix for the second version model

The average accuracy for the first version of the model using the COV-PEN dataset, with unfrozen layers, trained for 15 epochs with the Adam optimizer and a batch size of 128, is [please provide the accuracy percentage if known].

Table 5

Learning Rate	Ensemble Using Several Runs		
	Run 1	Run 2	Run 3
0.0002	0.815412186	0.843010753	0.842175627
0.0004	0.607526882	0.772401434	0.607526882
0.0006	0.866308244	0.798207885	0.81172043
0.0008	0.610394265	0.678853047	0.607526882
0.001	0.756630824	0.733333333	0.734050179

The average accuracy for the first version of the model using the COV-PEN dataset, with no frozen layers, trained for 15 epochs using the sigmoid optimizer and a batch size of 128, is [please provide the accuracy percentage if known].

Table 6

Learning Rate	Ensemble Using Several Runs		
	Run 1	Run 2	Run 3
0.0002	0.94265233	0.937275986	0.933691756
0.0004	0.933691756	0.908602151	0.919002151
0.0006	0.9390681	0.88172043	0.843010753
0.0008	0.935483871	0.869175627	0.81172043
0.001	0.734050179	0.790322581	0.756630824

The AUC (Area Under the Curve) of the receiver operating characteristic (ROC) curve, which plots true positives against false positives, was used to evaluate the diagnostic efficiency of the models. The AUC is calculated by integrating the areas of small trapezoidal fragments under the ROC curve. Figures 5 and 6 display the AUC evaluations for the proposed method, including the first edition (with no frozen layers and with the first 50 layers frozen) and the second version models. Figure 12 shows the AUC for the proposed first edition framework classification model, which achieves an AUC of 1, indicating perfect classification performance. This model slightly outperforms existing COVID-19 classification models.

Fig.8. ROC curve for first version model freeze =0

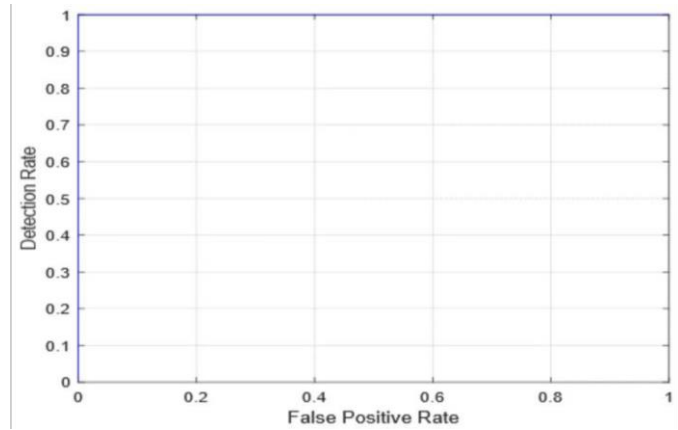


Fig.9. ROC curve for first version model freeze = 50

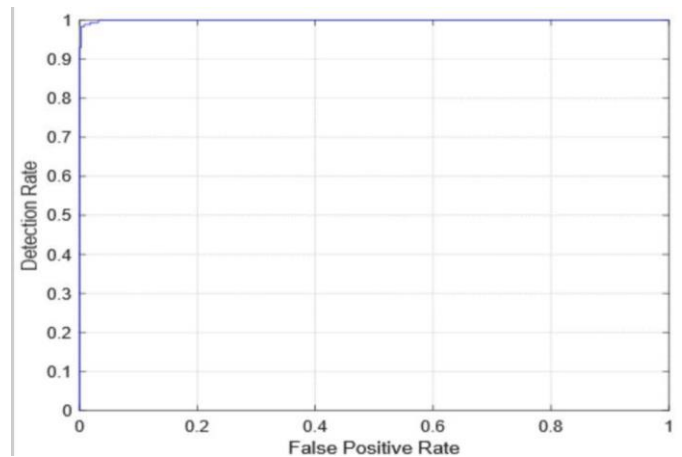


Fig.7. ROC curve for Second version model

Table 8 displays the optimal outcomes attained by employing the first version of the model with no frozen layers (freeze = 0), the first 50 layers frozen (freeze = 50), and the second version models. The performance discrepancy arises because the first version with freeze = 0 and the second version models feature an additional layer initialized with random weights instead of pre-trained weights, unlike the other layers. These random weights offer additional flexibility to the model, potentially improving its capacity for generalization.

Table 8

Quantitative Measures	1st Version Model (freeze = 0)	1st Version Model (freeze = 50)	2nd Version Model
Overall Accuracy	99.05	99.63	99.05
Precision	98.89	100	98.92
Recall	98.39	98.89	98.39
F1-score	98.63	99.44	98.65
AUC	99.99	100	99.98

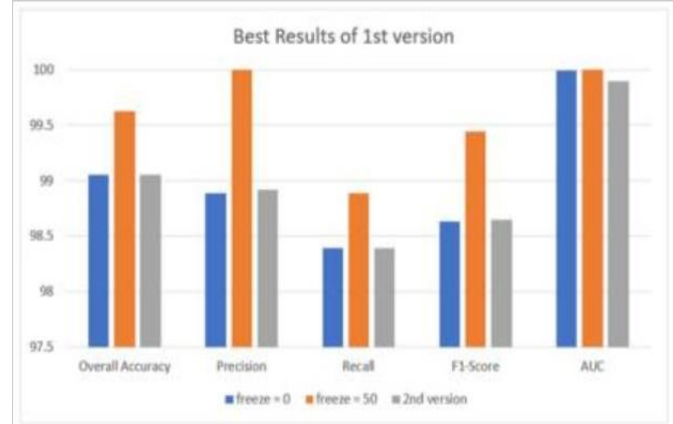


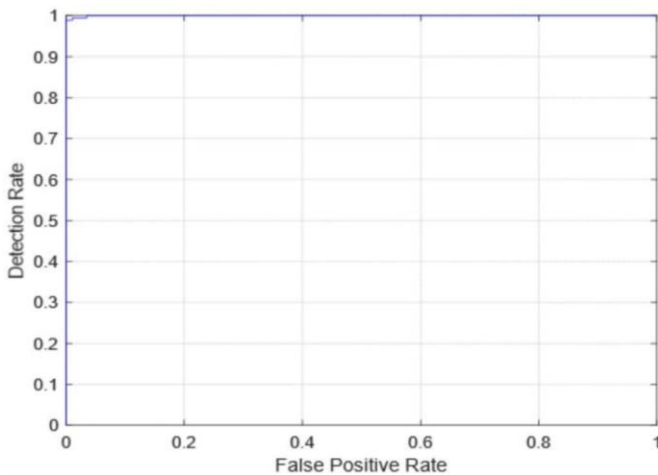
Table 8 depicts the optimal outcomes achieved in terms of overall accuracy, precision, recall, F1-score, and AUC. It shows that the best performance is attained when utilizing the first version of the model with freeze = 50.

The first version model was employed to compare the efficiency of the proposed COV-PEN scheme with current state-of-the-art approaches, highlighting its ability to leverage the strengths of each classifier. These findings support the implementation of the proposed COV-PEN method in real-world environments, aiding radiologists in more accurately diagnosing COVID-19 infections using CXR images while also reducing their workload.

5. Conclusion

A robust and automated COVID-19 diagnosis mechanism utilizing chest radiography images distinguishes between mild pneumonia and COVID-19 infections. The proposed system incorporates image enhancement techniques to enhance CXR image intensity and reduce noise. To enhance generalization and prevent overfitting, two variants of the ResNet-50 model were trained on preprocessed chest medical imaging.

The reliability of the system was evaluated on the COV-PEN dataset, achieving impressive metrics: an overall accuracy of 99.63%, precision of 100%, recall of 98.89%, F1-score of 99.44%, and an AUC



of 100%. These results indicate comparable performance to expert radiologists and outperform existing models based on comparative studies. Future work includes experiments with larger and more diverse datasets containing multiple COVID-19 cases to further validate the efficacy of the proposed system.

Potential extensions involve exploring other deep learning architectures such as DenseNet, VGG, or Inception-ResNet networks on the COV-PEN dataset, aiming to enhance diagnostic accuracy and robustness in COVID-19 detection from chest radiography images.

6. Reference

- Humayun M., Alsayat A. Prediction Model for Coronavirus Pandemic Using Deep Learning. *Comput. Syst. Sci. Eng.* 2022;40:947–961. doi: 10.32604/csse.2022.019288.
- Gorbalenya A.E., Baker S.C., Baric R., Groot R.J.d., Drosten C., Gulyaeva A.A., Haagmans B.L., Lauber C., Leontovich A.M., Neuman B.W., et al. Severe acute respiratory syndrome-related coronavirus: The species and its viruses—A statement of the Coronavirus Study Group. *bioRxiv*. 2020.
- Stoecklin S.B., Rolland P., Silue Y., Mailles A., Campese C., Simondon A., Mechain M., Meurice L., Nguyen M., Bassi C., et al. First cases of coronavirus disease 2019 (COVID-19) in France: Surveillance, investigations and control measures, January 2020. *Eurosurveillance*. 2020;25:2000094.
- Khalil M.I., Tehsin S., Humayun M., Jhanjhi N., Zain M.A. Multi-Scale Network for Thoracic Organs Segmentation. *Comput. Mater. Contin.* 2022;70:3251–3265. doi: 10.32604/cmc.2022.020561.
- Chavez S., Long B., Koyfman A., Liang S.Y. Coronavirus Disease (COVID-19): A primer for emergency physicians. *Am. J. Emerg. Med.* 2021;44:220–229. doi: 10.1016/j.ajem.2020.03.036.
- Al-Waisy A., Mohammed M.A., Al-Fahdawi S., Maashi M., Garcia-Zapirain B., Abdulkareem K.H., Mostafa S., Kumar N.M.,
Le D.N. Covid-deepnet: Hybrid multimodal deep learning system for improving covid-19 pneumonia detection in chest X-ray images. *Comput. Mater. Contin.* 2021;67:2409–2429. doi: 10.32604/cmc.2021.012955.
- Elghamrawy S.M., Hassnien A.E., Snasel V. Optimized Deep Learning-Inspired Model for the Diagnosis and Prediction of COVID-19. *Comput. Mater. Contin.* 2021;67:2353–2371. doi: 10.32604/cmc.2021.014767.
- Armstrong M. The Countries with the Most COVID-19 Cases. 2021. Available online: <https://www.statista.com/chart/21467/countries-most-covid-19-cases/> (accessed on 13 December 2021).
- Asai T. COVID-19: Accurate Interpretation of Diagnostic Tests—A Statistical Point of View. 2021. Available online: <https://www.ncbi.nlm.nih.gov/pmc/articles/PMC7729143/> [PMC free article] [PubMed] (accessed on 13 December 2021).
- Gaál G., Maga B., Lukács A. Attention u-net based adversarial architectures for chest X-ray lung segmentation. *arXiv*. 2020.2003.10304.